Int. J. Heat Mass Transfer. Vol. 34, No. 3, pp. 649–661, 1991
Printed in Great Britain

0017–9310/91 $3.00+0.00

Responses of concrete walls to fire

C. L. D. HUANG, GAMAL N. AHMED and D. L. FENTON
Department of Mechanical Engineering, Durland Hall, Kansas State University, Manhattan, KS 66506, U.S.A.

(*Received* 4 *October* 1989 *and in final form* 16 *April* 1990)

Abstract – Understanding the phenomena of coupled heat and mass transfer in concrete structures subject to high temperatures in a short duration has essential applications in the safety assessment of nuclear reactors and of tall buildings. In this paper a mathematical model, simulating the coupled heat and mass transfer in concrete structures at elevated temperatures as fire, has been developed and numerically solved. The numerical results predict the phenomenon of 'moisture clog' and the explosive spalling of concrete under fire. The investigations show that the seal layer as a fire protection has significant effects on the pore pressure buildup in the concrete walls which, in turn, improves the susceptibility of fire damage.

INTRODUCTION

OF GREAT concern in fire safety is the ability to determine the structural integrity of concrete buildings after a severe fire. Under such high temperature gradients, a strong coupling of heat and mass transfer mechanisms is involved in concrete. The knowledge of concrete behavior under fire, such as the changes in the pore pressure, temperature, and moisture in the structure with time as well as their distributions, is important in the safety considerations of concrete buildings.

Numerous studies in the literature consider the moisture transport in porous media induced by pore pressure gradients. Harmathy [1], Huang *et al.* [2, 3], among others, were interested in the hygrothermal behavior of concrete slabs with external conditions very close to those of the atmospheric surroundings. On the other hand, extreme conditions were investigated with respect to the safety of nuclear reactors or the behavior of materials subject to fires [4–16].

In recent analyses on concrete structures subject to elevated temperatures, moisture transfer was modeled on the basis of the evaporation–condensation mechanism driven by high pressure and moisture concentration gradients [6, 7]. These models have been tested with limited experimental data obtained elsewhere. Bažant and Thonguthai [8] developed a finite element model studying the coupled heat and mass transfer in concrete at high temperatures. Their numerical results of the moisture loss were compared with the test reported by Chapman and England [9]. Experimental studies on reinforced concrete columns were started a few years ago for the purpose of updating existing fire resistance ratings for columns [10, 11].

Harmathy [12] and Schneider [13] recently reported a condensed survey of the present state of knowledge and an outline of how much is already known in the field of high temperature properties of concrete.

Concrete contains a fine porous system filled with adsorbed and evaporable water. Under such high temperatures as in fires, convective and diffusive mass and heat transfer are involved simultaneously in concrete. Induced expansion of gases, such as water vapor and air, within the pores and evaporation of free water generate high pressure and concentration gradients. As a result, convective mass flow of gaseous mixture towards the heated and/or cold surfaces, driven by the pore pressure gradient, is developed. This convective mass flow of gases is the dominant mechanism in the transport phenomena. Diffusive mass flow developed by the concentration gradient may enhance the evaporation rates as well. The pore pressure buildup developed in concrete exposed to fire generates stresses that may exceed the yield strength, and hence explosive spalling of concrete may occur.

The problem of heat and mass transfer in concrete subject to high temperatures, such as in fires involves: strong coupling of pressure, temperature, and moisture content distributions, multiphase mass transfer (as liquid and gaseous phases), and highly non-linear dependence of various material parameters of porous media (such as permeability, conductivity, density, specific heats, and sorption curves, etc.) on temperature, pressure and moisture. Developing a mathematical model capable of rationally determining structural fire response and taking into account all the above factors and correctly simulating the heat and mass transfer in concrete is a complex process. Nevertheless, predicting the response of concrete structures to fire is of considerable concern for safety assessments. An accurate mathematical model is needed.

In this paper, a mathematical model, simulating the heat and mass transfer in concrete structures under fire, has been developed. This model provides for consideration of changes in pore pressure, temperature, and moisture, with corresponding changes in concrete properties, through the fire exposure period and the following decay period. For the purposes of fire safety, the models of concrete walls with a protecting seal

NOMENCLATURE

a_0 reference permeability [m s^{-1}]
C_P effective heat capacity [kJ kg^{-1} K^{-1}]
C_{Pi} specific heat of component i at constant pressure [kJ kg^{-1} K^{-1}]
D modified diffusivity of the gaseous mixture [m^2 s^{-1}]
D' diffusivity of gaseous mixture [m^2 s^{-1}]
e effective emissivity
h_c convective heat transfer coefficient [W m^{-2} K^{-1}]
h_D mass transfer coefficient [kmol m^{-2} s^{-1}]
h_{es} heat transfer coefficient of the side exposed to high temperatures [W m^{-2} K^{-1}]
h_{us} heat transfer coefficient of the side exposed to an atmospheric environment [W m^{-2} K^{-1}]
k effective thermal conductivity of the porous medium [W m^{-1} K^{-1}]
k_i thermal conductivity of component i of porous medium [W m^{-1} K^{-1}]
k_g thermal conductivity of the gaseous mixture [W m^{-1} K^{-1}]
K_D Darcy's coefficient or coefficient of permeability [m^3 s^{-1} kg^{-1}]
m volumetric moisture content per unit volume of the porous system [m^3 m^{-3}]
M molecular weight of the gaseous mixture [kg kmol^{-1}]
M_i molecular weight of component i of the gaseous mixture [kg kmol^{-1}]
P total pressure or pore pressure [N m^{-2}]
Q latent heat of evaporation of free water [kJ kg^{-1}]
R universal gas constant [kJ kmol^{-1} K^{-1}]
t time [s]
T absolute temperature [K]
V_g bulk velocity of the gaseous mixture [m s^{-1}]
w/c free water–cement ratio [kg kg^{-1}]
x space coordinate.

Greek symbols

Γ mass rate of evaporation per unit volume of the porous system [kg m^{-3} s^{-1}]
ε porosity of the porous system
ε_g volume fraction of the gaseous mixture [m^3 m^{-3}]
ρ effective density of the porous system [kg m^{-3}]
ρ_i density of component i [kg m^{-3}]
σ Stefan–Boltzman constant [W m^{-2} K^{-4}]
ϕ mole fraction of water vapor of the gaseous mixture [kmol kmol^{-1}].

Subscripts

atm atmosphere
es at the exposed surfaces to fire
f fire
g gaseous mixture
i component i of the porous system
l liquid
s at the surface
us at the unexposed surfaces to fire
v vapor in a gaseous mixture
w water
0 initial condition or datum
∞ ambient.

layer on their fire exposed surfaces and without the protecting layer are developed and analyzed. The ASTM E119 code is used to describe the developing period of the fire exposure, while the following decay period follows ISO 834 standard.

GOVERNING EQUATIONS

A mathematical model describing the coupled heat and mass transfer in porous media, such as concrete, is derived. As with any such approach, certain assumptions need to be made to provide a model which is suitably efficient for both design and analysis applications. Consequently, the following assumptions concerning the porous system and the transport process are introduced: a multi-phase porous system is taken as a continuous medium, local thermodynamic equilibrium exists, a rigid solid matrix and incompressible liquid are assumed, mobility of liquid is assumed to be negligible as compared to that of gaseous mixtures; water vapor, air, and their mixture are ideal gases; compressional work and viscous dissipation are negligible; and energy transferred by diffusion compared to conduction is negligible.

Given such assumptions and based on the concepts of continuum mechanics, principles of irreversible thermodynamics; and conservation of mass, momenta, and energy equations, a set of three basic equations are derived as follows:

Conservation of mass for water liquid

$$\frac{\partial}{\partial t}\rho w(\varepsilon-\varepsilon_g) = -\Gamma. \tag{1}$$

Conservation of mass for water vapor

$$\rho_v\varepsilon_g\frac{\partial\phi}{\partial t} - (1-\phi)\Gamma = -\rho_v\varepsilon_g V_g\cdot\nabla\phi + \frac{\rho_g}{\rho_a}\nabla\cdot(\rho_g\varepsilon_g D\nabla\phi) \tag{2}$$

where

$$D = M_w M_a D'/M^2 = D(\phi).$$

Conservation of mass for air component

$$-\rho_v \varepsilon_g \frac{\partial \phi}{\partial t} + (1-\phi)\Gamma = \rho_v \varepsilon_g V_g \cdot \nabla \phi - \frac{\rho_g}{\rho_a} \nabla \cdot (\rho_g \varepsilon_g D \nabla \phi). \quad (3)$$

Conservation of mass for gaseous mixture

$$\frac{\partial}{\partial t}(\rho_g \varepsilon_g) + \nabla \cdot (\rho_g \varepsilon_g V_g) = \Gamma. \quad (4)$$

Conservation of energy equation

$$\rho c_P \frac{\partial T}{\partial t} + \rho_w Q \frac{\partial \varepsilon_g}{\partial t} = \nabla \cdot (k \nabla T) - \rho_g \varepsilon_g C_{Pg} V_g \cdot \nabla T. \quad (5)$$

The moisture content, m, is related to the pore pressure, P, temperature, T, and mole fraction of water vapor in the gaseous mixture, ϕ, through a state equation, i.e. $m = m(P, T, \phi)$. This constitutive relation is given as a set of sorption isotherms for various temperatures of concrete through experimental techniques [8]. With the definition of the volume fraction of gaseous mixture, $\varepsilon_g = \varepsilon - m(P, T, \phi)$,

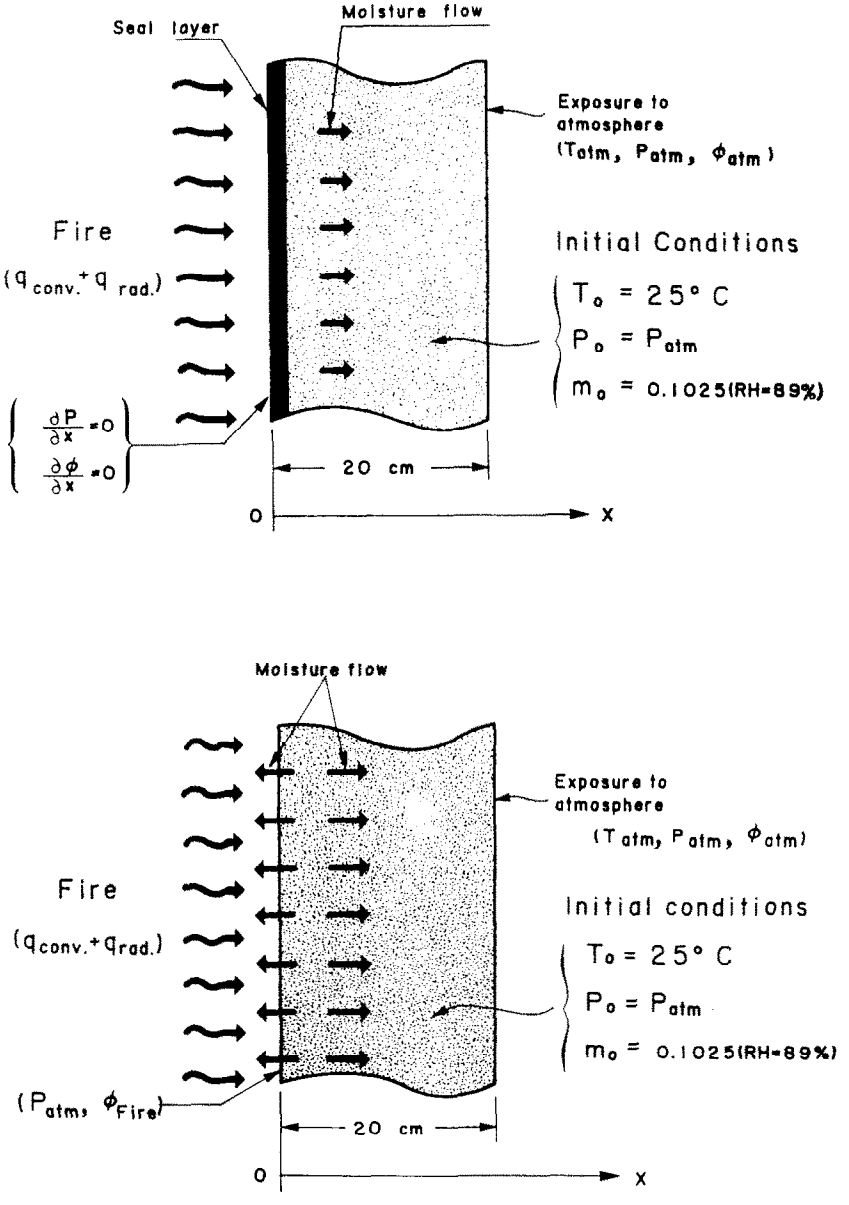

FIG. 1. Sealed and unsealed concrete slabs under fire.

Table 1. Values of the physical properties and coefficients

Symbol	Value	Unit
a_0	1.1×10^{-12}	m s^{-1}
k_d	1.88	W m^{-1} K^{-1}
$(\rho c_P)_d$	1.825×10^{3}	kJ m^{-3} K^{-1}
w/c	0.34	kg kg^{-1}
ε	0.16	
e	0.9	
σ	5.669×10^{-8}	W m^{-2} K^{-4}
D_f	10800.0	s
M_w	18.016	kg kmol^{-1}
M_a	28.952	kg kmol^{-1}
R	8.3143	kJ kmol^{-1} K^{-1}
$h_{c,cs}$	50.0	W m^{-2} K^{-1}
$h_{c,us}$	10.0	W m^{-2} K^{-1}
$h_{D,us}$	$(1.0\times10^{-7}\ 18.84\times10^{-4})$	kmol m^{-2} s^{-1}
ϕ_∞	0.0118754	kmol kmol^{-1}
P_{atm}	1.01325×10^{5}	N m^{-2}
T_∞	298	K

a set of three coupled non-linear second-order partial differential equations is obtained. For one-dimensional heat and mass transfer in a concrete slab of thickness L, this set of equations is of the form

$$A_k\frac{\partial\phi}{\partial t}+B_k\frac{\partial P}{\partial t}+C_k\frac{\partial T}{\partial t}=D_k\frac{\partial^2\phi}{\partial x^2}+E_k\frac{\partial^2 P}{\partial x^2}+F_k\frac{\partial^2 T}{\partial x^2}+G_k\left(\frac{\partial\phi}{\partial x}\right)^2+H_k\left(\frac{\partial P}{\partial x}\right)^2+I_k\left(\frac{\partial T}{\partial x}\right)^2+J_k\left(\frac{\partial\phi}{\partial x}\frac{\partial P}{\partial x}\right)+K_k\left(\frac{\partial\phi}{\partial x}\frac{\partial T}{\partial x}\right)+L_k\left(\frac{\partial P}{\partial x}\frac{\partial T}{\partial x}\right) \quad (6)$$

where the coefficients $A_k,\ldots,L_k$ for $k=1, 2, 3$ are functions of the dependent variables ϕ, P, and T. They are defined as follows:

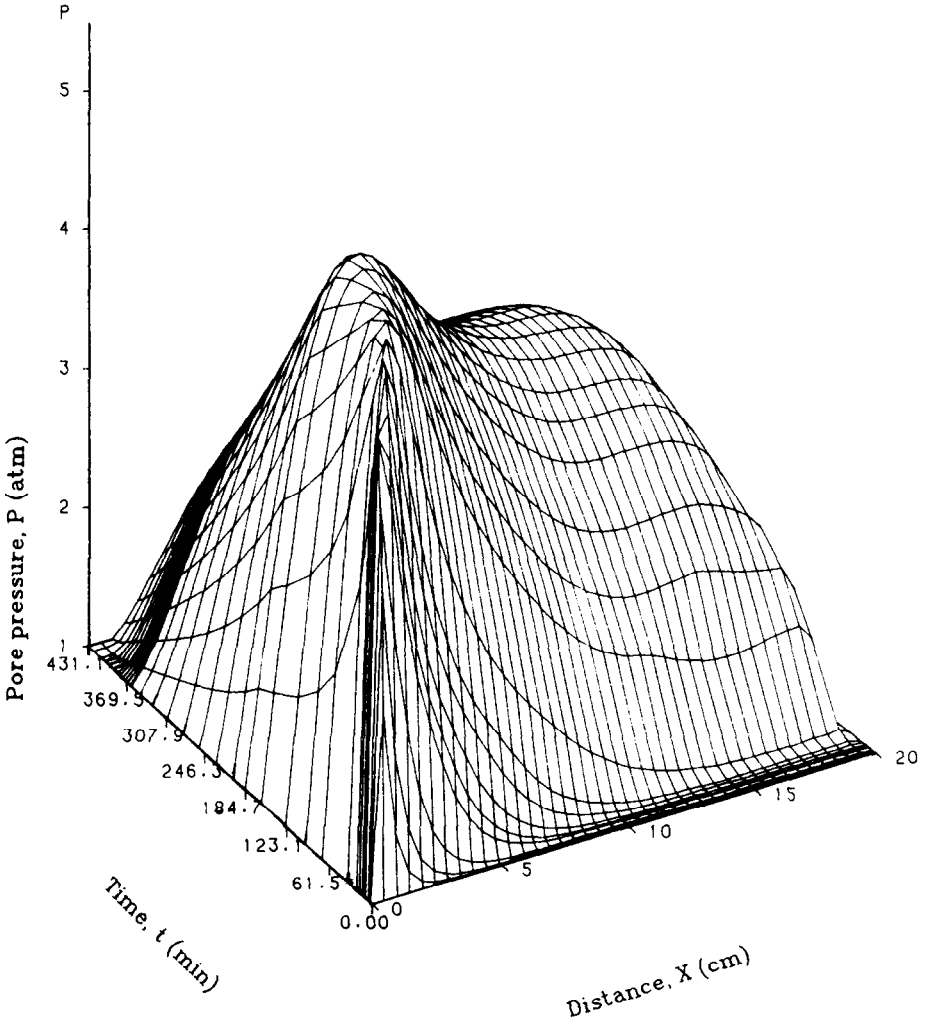

FIG. 2. Pore pressure as a function of depth and time for unsealed concrete slab under fire.

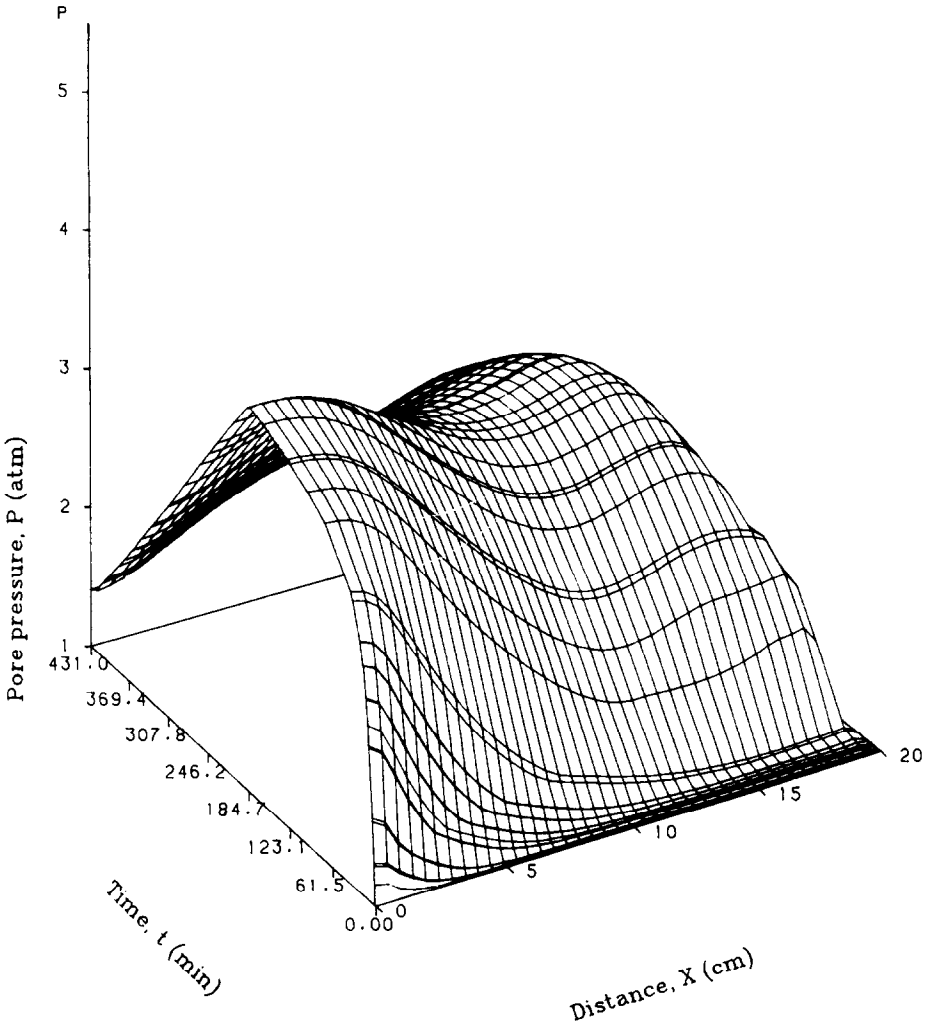

FIG. 3. Pore pressure as a function of depth and time for sealed concrete slab under fire.

$$A_1 = 1-\left(\frac{(1-\phi)\rho_w}{(PM_w/RT)}\frac{1}{\varepsilon_g}\frac{\partial\varepsilon_g}{\partial\phi}\right), \qquad A_2 = \left(1-\frac{\rho_w}{PM/RT}\right)\frac{1}{\varepsilon_g}\frac{\partial\varepsilon_g}{\partial\phi}+\frac{M_w-M_a}{M}$$

$$B_1 = -\left(\frac{(1-\phi)\rho_w}{(PM_w/RT)}\frac{1}{\varepsilon_g}\frac{\partial\varepsilon_g}{\partial P}\right), \qquad B_2 = \left(1-\frac{\rho_w}{PM/RT}\right)\frac{1}{\varepsilon_g}\frac{\partial\varepsilon_g}{\partial P}+\frac{1}{P}$$

$$C_1 = -\left(\frac{(1-\phi)\rho_w}{(PM_w/RT)}\frac{1}{\varepsilon_g}\frac{\partial\varepsilon_g}{\partial T}\right), \qquad C_2 = \left(1-\frac{\rho_w}{PM/RT}\right)\frac{1}{\varepsilon_g}\frac{\partial\varepsilon_g}{\partial T}-\frac{1}{T}$$

$$D_1 = D', \quad D_2 = 0$$
$$E_1 = 0, \quad E_2 = K_D$$
$$F_1 = 0, \quad F_2 = 0$$

$$G_1 = D'\left(\frac{1}{\varepsilon_g}\frac{\partial\varepsilon_g}{\partial\phi}-\frac{M_w-M_a}{M}\right), \quad G_2 = 0$$

$$H_1 = 0, \quad H_2 = \frac{\partial K_D}{\partial P}+K_D\left(\frac{1}{\varepsilon_g}\frac{\partial\varepsilon_g}{\partial P}+\frac{1}{P}\right)$$

$$I_1 = 0, \quad I_2 = 0$$

$$J_1 = D'\left(\frac{1}{\varepsilon_g}\frac{\partial\varepsilon_g}{\partial P}+\frac{1}{P}\right)+K_D, \qquad J_2 = \frac{\partial K_D}{\partial\phi}+K_D\left(\frac{1}{\varepsilon_g}\frac{\partial\varepsilon_g}{\partial\phi}+\frac{M_w-M_a}{M}\right)$$

$$K_1 = D'\left(\frac{1}{\varepsilon_g}\frac{\partial\varepsilon_g}{\partial T}-\frac{1}{T}\right), \quad K_2 = 0$$

$$L_1 = 0, \quad L_2 = \frac{\partial K_D}{\partial T}+K_D\left(\frac{1}{\varepsilon_g}\frac{\partial\varepsilon_g}{\partial T}-\frac{1}{T}\right)$$

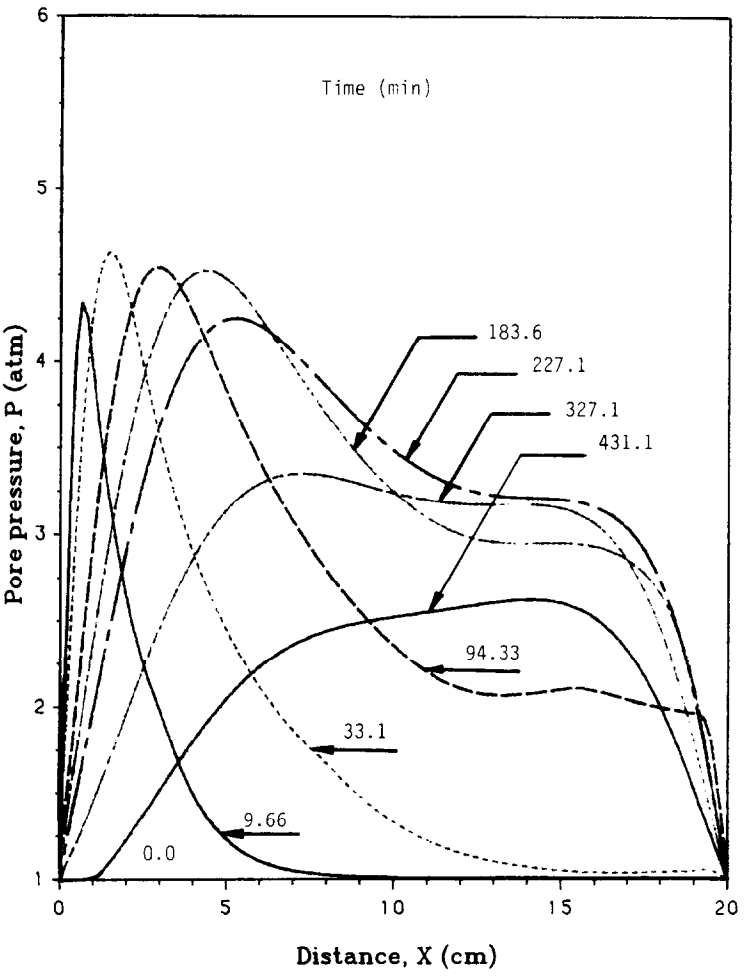

FIG. 4. Pore pressure distributions in unsealed concrete slab under fire.

$$A_3 = \rho_w Q \frac{\partial \varepsilon_g}{\partial \phi}, \quad G_3 = 0$$

$$B_3 = \rho_w Q \frac{\partial \varepsilon_g}{\partial P}, \quad H_3 = 0$$

$$C_3 = \rho_w Q \frac{\partial \varepsilon_g}{\partial T} + \rho C_P, \quad I_3 = k' \frac{\partial \varepsilon_g}{\partial T}$$

$$D_3 = 0, \quad J_3 = 0$$

$$E_3 = 0, \quad K_3 = k' \frac{\partial \varepsilon_g}{\partial \phi}$$

$$F_3 = k(\varepsilon_g), \quad L_3 = k' \frac{\partial \varepsilon_g}{\partial P} + K_D(\rho_g \varepsilon_g C_{Pg})$$

$$M = \phi M_w + (1-\phi) M_a = M(\phi)$$

$$\rho C_P = (1-\varepsilon)\rho_s C_{Ps} + (\varepsilon - \varepsilon_g)\rho_w C_{Pw} + \rho_g \varepsilon_g C_{Pg}$$

$$k' = \frac{\mathrm{d}k(\varepsilon_g)}{\mathrm{d}\varepsilon_g}$$

$$k(\varepsilon_g) = [(1-\varepsilon)k_s^{1/4} + (\varepsilon - \varepsilon_g)k_L^{1/4} + \varepsilon_g k_g^{1/4}]^4.$$

BOUNDARY CONDITIONS AND INITIAL CONDITIONS

Consider one-dimensional sealed and unsealed concrete slabs exposed to fire as shown schematically in Fig. 1. One surface of the slab ($x = 0$) is exposed to fire, on which a protecting seal layer may or may not be installed. The temperature course of the fire may be divided into two periods: developing period and decay period. The fire temperature course in the developing period is assumed to follow that of the standard fire described in ASTM E-119 over a fire exposure duration of 3 h. After the fire exposure, the fire temperature in the following decay period is assumed to decrease linearly to the atmospheric temperature according to the relations specified in ISO 834 standard. Depending on the fire exposure duration; the longer the duration of the developing period, the lower the rate of decrease of temperature in the decay period [11, 14]. The other surface of the concrete slabs ($x = L$) remains under regular atmospheric conditions, with that the heat and mass are transferred

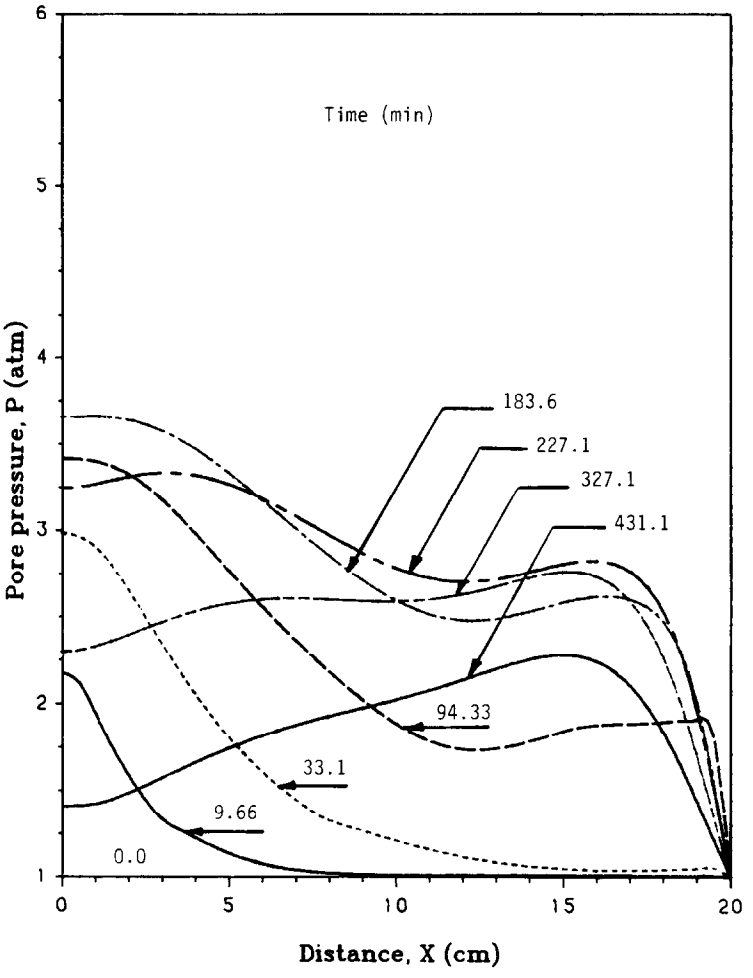

FIG. 5. Pore pressure distributions in sealed concrete slab under fire.

freely through the surface to the surroundings. Thus, the boundary conditions are described as

at $x = 0$:

unsealed concrete slabs	*sealed concrete slab*	
$P = P_{atm}$	$\dfrac{\partial P}{\partial x} = 0$	(7)
$\phi = \phi_f = 0$	$\dfrac{\partial \phi}{\partial x} = 0$	(8)

$$-k\frac{\partial T}{\partial x} = h_{es}(T_f(t) - T) \text{ for both cases} \tag{9}$$

where

$$h_{es} = h_{c,es} + e\sigma(T_f(t) + T)(T_f(t)^2 + T^2);$$

at $x = L$: for both sealed and unsealed concrete slabs

$$P = P_{atm} \tag{10}$$

$$-k\frac{\partial T}{\partial x} = h_{us}(T - T_\infty) \tag{11}$$

$$-\left(\frac{P_{atm}D'}{RT}\right)\frac{\partial \phi}{\partial x} = h_D(\phi - \phi_\infty) \tag{12}$$

where

$$h_{us} = h_{c,us} + e\sigma(T_\infty + T)(T_\infty^2 + T^2).$$

The initial conditions used in this study are given as

$$P(x,0) = P_{atm}, \quad T(x,0) = T_0, \quad \phi(x,0) = \phi_0. \tag{13}$$

Equations (6)–(13) form a complete mathematical model for the coupled heat and mass transfer in sealed and unsealed concrete slabs under fire. The physical properties and coefficients along with the boundary and initial conditions for the cases considered in this study are given in Table 1.

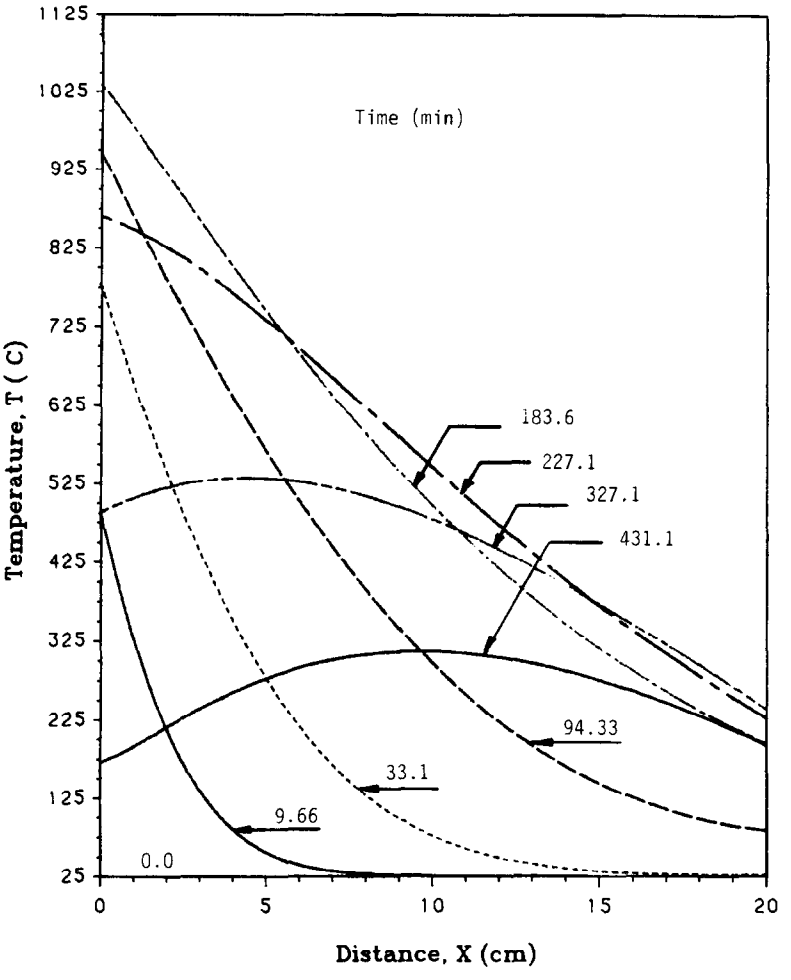

FIG. 6. Temperature distributions in both sealed and unsealed concrete slabs under fire.

NUMERICAL METHOD

The present work seeks to develop an efficient numerical procedure for solving this coupled set of basic equations (6)–(13). These equations can be expressed in general form in terms of a dependent variable, $U_k, k = 1, 2, 3$. U_1, U_2, and U_3, representing mole fraction of water vapor in the gaseous mixture, ϕ, pore pressure, P, and temperature, T, are functions of space, x, and time, t.

A fully implicit finite difference scheme incorporating quasi-linearization of the non-linear coefficients and the mixed derivatives is employed. First, the non-linear coefficients, $A_k, \ldots, L_k$, are quasi-linearized by evaluating all these coefficients at time, t_n. This is known as 'lagging' the coefficients. Then using a simple iterative updating procedure, these coefficients can be ultimately evaluated at t_{n+1} as required. To do this, the coefficients are first evaluated at the nth lagged level and the system is solved for new values of U_k, $k = 1, 2, 3$, at the $(n+1)$th level. The coefficients can then be updated by utilizing the solution just obtained at the $(n+1)$th level. The calculation is repeated to obtain a better prediction at this level. This procedure can be repeated iteratively until changes are sufficiently small. Usually only two or three iterations are used.

Second, the time derivatives, $\partial U_k/\partial t$, are replaced by first-order forward finite difference in time. While the derivatives $\partial U_k/\partial x$ and $\partial^2 U_k/\partial x^2$ are replaced by fully implicit central finite difference of first- and second-order accurate in space respectively at the new time level, $t_{n+1} = t_n + \Delta t$. In quasi-linearization of the mixed derivatives, $(\partial U_k/\partial x)(\partial U_j/\partial x)$ where $k, j = 1, 2, 3$, a Newton linearization with coupling is applied to the fully implicit finite difference representation of these mixed derivatives and is given as follows:

$$\left(\frac{\partial U_k}{\partial x}\frac{\partial U_j}{\partial x}\right)_i^{n+1} \cong \left(\frac{\partial U_j}{\partial x}\right)_i^{n}\left(\frac{\partial U_k}{\partial x}\right)_i^{n+1} + \left(\frac{\partial U_k}{\partial x}\right)_i^{n}\left(\frac{\partial U_j}{\partial x}\right)_i^{n+1} - \left(\frac{\partial U_k}{\partial x}\frac{\partial U_j}{\partial x}\right)_i^{n}$$

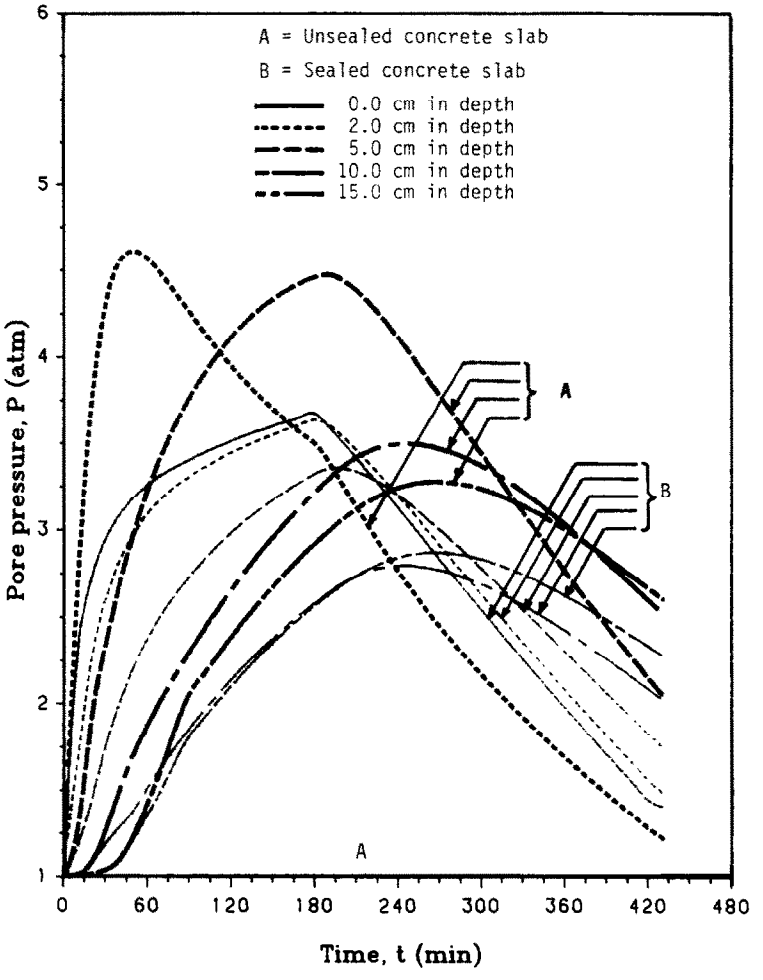

FIG. 7. Pore pressure history in sealed and unsealed concrete slabs at various depths.

$$\cong \frac{1}{(2\Delta x)^2}((-U^n_{j,i-1}+U^n_{j,i+1})(-U^{n+1}_{k,i-1}+U^{n+1}_{k,i+1}) + (-U^n_{k,i-1}+U^n_{k,i+1})(-U^{n+1}_{j,i-1}+U^{n+1}_{j,i+1}) - (-U^n_{k,i-1}+U^n_{k,i+1})(-U^n_{j,i-1}+U^n_{j,i+1})). \quad (14)$$

Coupling the discrete boundary conditions with the set of implicit finite difference equations, after being quasi-linearized, results in a three-by-three block-tridiagonal system of equations in the form $\hat{A}\,\hat{U} = \hat{R}$ where $\hat{A}$ is a $3(N-2)\times 3(N-2)$ sparse unsymmetric matrix, $\hat{U}$ and $\hat{R}$ are $3(N-2)$ vectors with N being the number of nodes in the x-direction.

This system of linearized equations has been solved efficiently by MA28, a set of FORTRAN subroutines for the solution of sparse unsymmetric linear equations using a variant of Gaussian elimination [15].

To minimize the computing time and control the truncation errors, a time-step has to be chosen to be smaller than the transient time scale of the phase change. In other words, the larger the moisture content in the porous medium, the smaller the time-step used. At the beginning of computation, a smaller time-step should be chosen than that at the advanced stages of computation (Δt ranges from 0.1 to 120 s). Therefore, the adjustment of the value of Δt must be carried out periodically to keep $\|\Delta\varepsilon_{g,i}\|_2 < \varepsilon_c$ where ε_c is a small value. The limit on $\|\Delta\varepsilon_{g,i}\|_2$ controls the truncation errors, because ε_g is a function of the three dependent variables, U_1, U_2, and U_3. Numerical results are shown in Figs. 2–9.

RESULTS AND DISCUSSION

The histories of pore pressure distribution in both sealed and unsealed concrete slabs under aforementioned boundary conditions are given in Figs. 2 and 3. As can be inferred from these figures, the maximum pressure buildup occurs at/beneath the fire exposed surface of sealed and unsealed concrete slabs. The pressure peaks in sealed slabs are lower and the pressure penetration is slower than those in unsealed ones.

Figures 4 and 5 exhibit the spatial pore pressure distributions at different times in sealed and unsealed

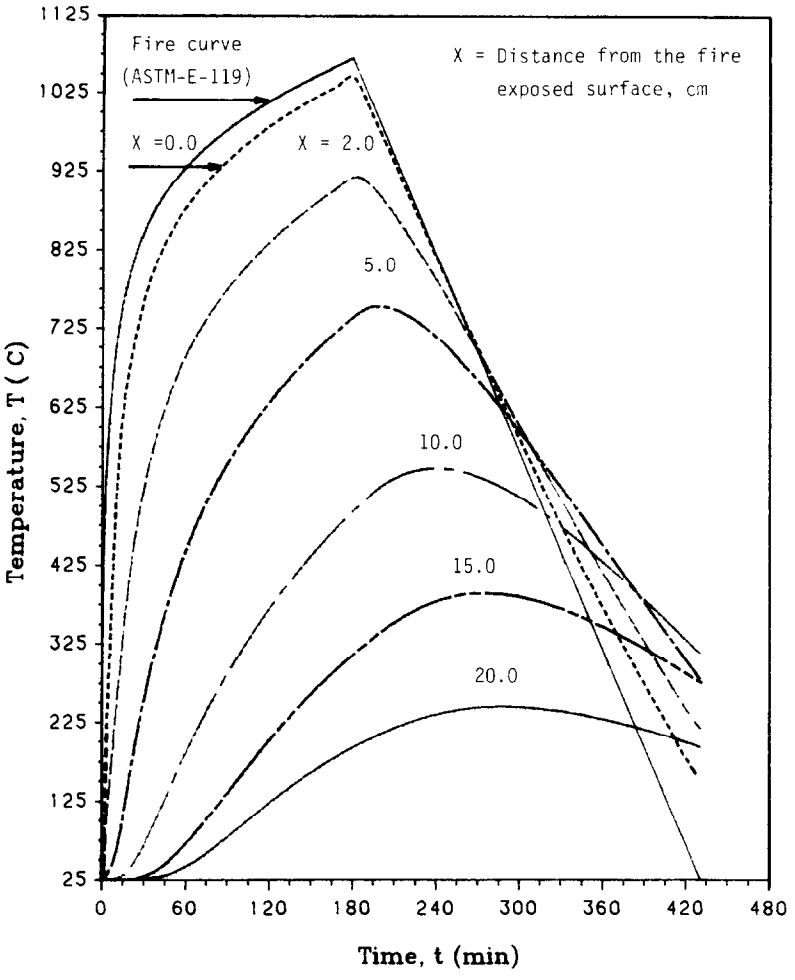

FIG. 8. Temperature history in sealed and unsealed concrete slabs at various depths.

concrete slabs. In both cases, the pressure builds up rapidly across the drying region as a result of high heat flux and low mass transport capacity of the heated concrete during the developing period of fire exposure which ranges from 0 to 3 h. By the movement of the drying front towards the cooler zones and during the decay period of fire, the pore pressure tends to dissipate or level off. As can be seen from these results significantly lower pressures can be expected in a sealed concrete slab as compared to an unsealed one. In addition, the pressure penetration into the sealed slab is slower than that into the unsealed one, e.g. at a depth of 1.5 cm and a time of 33.1 min, $P = 2.8$ atm for the sealed slab and 4.63 atm for the unsealed one.

In an unsealed concrete slab, the pressure peaks penetrate into the slab towards the cooler zones with time. Also, the rising branches of the pore pressure show steeper pressure gradients developed than the downward branches. Therefore, the steeper pressure gradients tend to drive more moisture towards the fire exposed surface to be released than the other surface. On the other hand, the pressure peaks developed in a sealed concrete slab are stationary at the sealed surface. Consequently, the pressure gradients tend to drive moisture only into the wall towards the cooler zones to be released from the surface exposed to atmospheric conditions.

The corresponding spatial temperature distribution at various times in both sealed and unsealed concrete slabs are given in Fig. 6. It is obvious that very steep temperature beneath the fire exposed surface in the early stages of fire indicates a high rate of heat transfer. This steep temperature gradient penetrates into the wall with time. In the wet region, away from the heated surface, the temperature gradients are reduced as a result of better thermal conductivity. Therefore, the heat transfer is enhanced by the evaporation–condensation mechanism. While the temperature distributions exhibit conductive transient phenomena, it seems that the seal layer does not have an effect on the temperature distributions. The same characteristics of pressure rise and fall as well as the temperature distribution in the porous system under high heat flux were also seen in other investigations [5, 8].

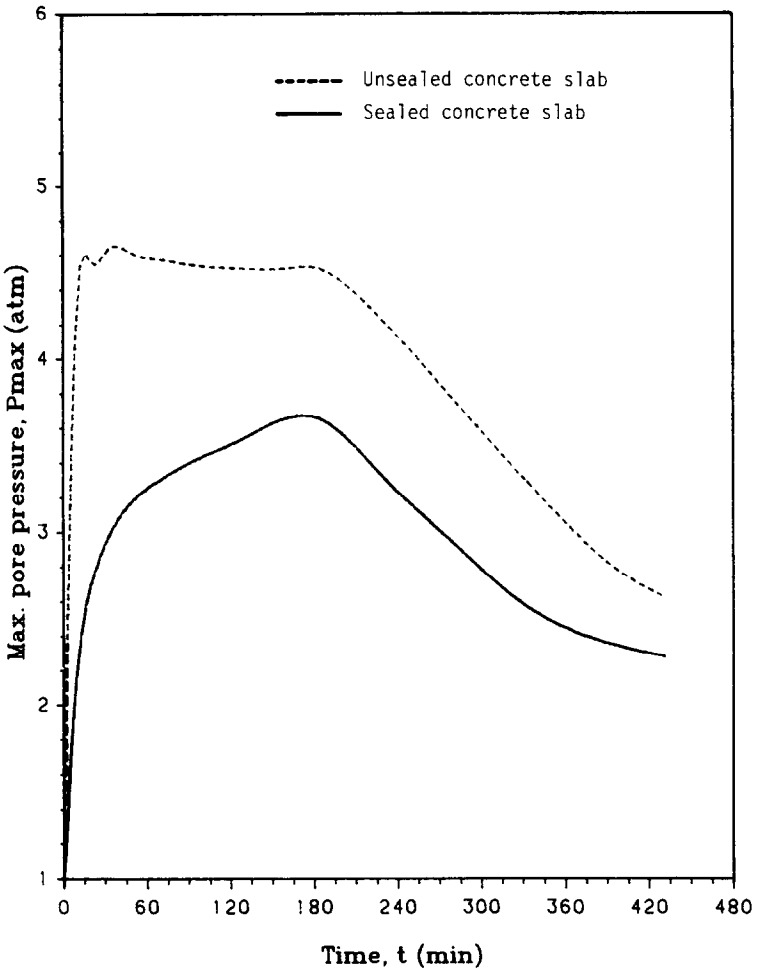

FIG. 9. Maximum pressure history in sealed and unsealed concrete slabs under fire.

In the early stages of fire exposure, a high heat flux penetrates into the concrete slab causing evaporation of the free water within the pores. A dry layer under the fire exposed surface is developed as a result of flowing a major portion of the moisture vapor towards the colder regions. At the same time, the moisture vapor accumulates in a neighboring layer next to the dry region. As the thickness of the dry layer increases, a highly saturated layer of considerable thickness, called a moisture clog, forms at some distance from the fire exposed surface. Having low mass transport capacity and steep temperature gradients, the pore pressure builds up rapidly at the drying front. Under such a high pressure gradient, a convective mass of gaseous mixture flowing towards both the heated and/or cold surface is developed. As a result, the moisture clog begins to move towards the colder regions and, then the pressure in the clog region soon levels off. Such a phenomenon is more pronounced in the case of an unsealed concrete slab than the sealed one as shown in Figs. 4 and 5. Therefore, due to a moisture clog and steep pressure gradient, explosive spalling of concrete is expected in the early stages of the fire when the pore pressure exceeds the ultimate tensile strength of the concrete. This phenomenon of moisture clog has been discussed by Harmathy [16].

Figures 7 and 8 show the evolution of pore pressure and temperature as functions of time at different depths for both sealed and unsealed concrete slabs. Figure 9 illustrates the effect of protecting the seal layer on the maximum pore pressure buildup with time as well. As can be seen from Fig. 7, the rate of pressure buildup in an unsealed concrete slab is higher than that in a sealed one. This continues until the pressure buildup reaches a maximum value, which occurs earlier in an unsealed slab than in a sealed one. In other words, the maximum pressure buildup in an unsealed slab occurs in early stages of the fire exposure and continues throughout the developing period and early stages of the decay period. While in a sealed one, it takes place during the later stages of the developing period and continues during the early stages of the following decay period. The maximum values of the pressure achieved are lower in a sealed slab than those

in an unsealed one. These results are substantiated by Fig. 9. As can be seen from these figures the effect of seal layer on the pore pressure buildup is more pronounced in the concrete zones closer to the fire exposed surface. In both cases of slabs, the pressure dissipates with time during the developing period of fire exposure and/or the following decay period since the vaporization in the heated zones has been completed, i.e. the dry concrete zone is comparatively permeable. Figure 8 exhibits the temperature response of concrete slabs to the fire exposure and the following decay period. The rate of temperature change is faster in the vicinity of the exposed surface of the concrete walls to fire.

CONCLUSIONS

The numerical results as shown precisely predict the phenomenon of 'moisture clog' during the fire exposure. It has also been shown that the temperature distributions in both sealed and unsealed concrete slabs exhibit conductive transient phenomena. As can be seen from these results the pressure in the elevated temperature zones is much higher than in cooler ones. Therefore, the convective gaseous mass flow, driven by pore pressure gradients, is the dominant mechanism in the transport phenomena, while the diffusion mechanism is more influential in the cooler zones of concrete slabs.

The investigations demonstrate that the seal layer as a fire protection has significant effects on the pore pressure buildup in concrete walls. As can be seen from the numerical results, the seal layer reduces and delays the pressure buildup which, in turn, improves the susceptibility of fire damages. The explosive spalling of concrete walls under fire can be avoided as long as the proper seal is provided and which limits the pore pressure under a safe level, well below the yield strength of the concrete.

REFERENCES

1. T. Z. Harmathy, Moisture and heat transport with particular reference to concrete, National Research of Canada, NRCC 12143, Canada (1971).
2. C. L. D. Huang, H. H. Siang and C. H. Best, Heat and moisture transfer in concrete slabs, *Int. J. Heat Mass Transfer* **22**, 252–266 (1979).
3. C. L. D. Huang, Multi-phase moisture transfer in porous media subject to temperature gradient, *Int. J. Heat Mass Transfer* **22**, 1295–1307 (1979).
4. G. O. England and T. J. Sharp, Migration of moisture and pore pressures in heated concrete, 1st Int. Conf. on Structural Mechanics in Reactor Technol., H2/4, pp. 129–143 (1971).
5. G. Dhatt, M. Jacquemier and C. Kadje, Modelling of drying refractory concrete, *Drying 86, Proc. 5th Int. Symp. on Drying*, McGill University, pp. 94–104 (1986).
6. M. S. Sahota and P. J. Pagni, Heat and mass transfer in porous media subject to fires, *Int. J. Heat Mass Transfer* **22**, 1069–1081 (1979).
7. A. Dayan and E. L. Gleukler, Heat and mass transfer within an intensely heated concrete slab, *Int. J. Heat Mass Transfer* **25**, 1461–1467 (1982).
8. Z. P. Bažant and W. Thonguthai, Pore pressure in heated concrete walls—theoretical prediction, *Mag. Concr. Res.* **31**(107), 67–76 (1979).
9. D. A. Chapman and G. L. England, Effects of moisture migration on shrinkage, pore pressure, and other concrete properties, Trans. 4th Int. Conf. on Structural Mechanics in Reactor Technol., H5/3, pp. 1–14 (1977).
10. T. T. Lie and T. D. Lin, *Fire Performance of Reinforced Concrete Columns, Fire Safety: Science and Engineering* (Edited by T. Z. Harmathy), ASTM STP 882, pp. 176–205. American Society for Testing and Materials, Philadelphia (1985).
11. T. T. Lie, T. J. Rowe and T. D. Lin, Residual strength of fire-exposed reinforced concrete columns, evaluation and repair of fire damage to concrete, American Concrete Institute, SP 92-9, pp. 153–174 (1986).
12. T. Z. Harmathy, Properties of building materials: bases for fire safety design. In *Design of Structures against Fire* (Edited by R. D. Anchor, H. L. Malhotra and J. A. Purkiss), pp. 87–105. Elsevier Applied Science (1986).
13. U. Schneider, Properties of materials at high temperatures. In *Concrete*, Department of Civil Engineering, 2nd Edn. University of Kassell, Kassell, Germany (1986).
14. T. T. Lie, Fire temperature–time relations. In *The SFPE Handbook of Fire Protection Engineering*, Section 3, Chap. 5, pp. 3-81–3-87 (JRC Paper No. 1579) (1988).
15. I. S. Duff, MA28—a set of FORTRAN subroutines for sparse unsymmetric linear equations, Computer Science and Systems Division, AERE Harwell (1980).
16. T. Z. Harmathy, Effect of moisture on the fire endurance of building elements, ASTM, Special Technical Publication No. 385, pp. 74–95 (1965).

REPONSE AU FEU DES MURS EN BETON

Résumé—La compréhension des phénomènes couplés de transfert de chaleur et de masse dans des structures en béton soumises à des températures élevées pendant un temps court est essentielle dans l'évaluation de la sécurité dans les réacteurs nucléaires et les grands immeubles. On développe et résout numériquement un modèle mathématique qui simule le transfert couplé de chaleur et de masse. Les résultats numériques prédisent le phénomène de blocage d'humidité et le délitement explosif du béton au feu. L'étude montre que la couche de protection a des effets significatifs sur l'accroissement de pression dans les pores du béton ce qui améliore la susceptiblité aux dégats causés par le feu.

DAS VERHALTEN VON BETONWÄNDEN IN FEUER

Zusammenfassung—Das Verständnis der Vorgänge beim gekoppelten Wärme- und Stofftransport in Betonstrukturen, die kurzzeitig hohen Temperaturen ausgesetzt sind, findet wesentliche Anwendungen bei Sicherheitsüberlegungen in Kernreaktoren und im Hochbau. In dieser Arbeit wird ein mathematisches Modell entwickelt und numerisch gelöst, das den gekoppelten Wärme- und Stofftransport in Betonstrukturen bei erhöhten Temperaturen (bzw. bei Feuer) simuliert. Die numerischen Ergebnisse zeigen das Phänomen der "Feuchtigkeitssperre" und das explosive Abplatzen von Beton im Feuer. Die Untersuchungen zeigen, daß eine schmelzbare Schicht als Feuerschutz wesentliche Einflüsse auf den Aufbau eines Drucks in den Poren von Betonwänden hat. Dies wiederum verbessert die Empfindlichkeit gegenüber feuerbedingten Schäden.

РЕАКЦИЯ БЕТОННЫХ СТЕН НА ОГОНЬ

Аннотация—Понимание явлений взаимосвязанного тепло- и массопереноса в бетонных структурах, подверженных кратковременному воздействию высоких температур, находит важное применение в оценке безопасности ядерных реакторов и высоких зданий. В данной работе разрабатывается и численно решается математическая модель, описывающая сложный тепло- и массоперенос в бетонных структурах при высоких температурах, соответствующих возгоранию при пожаре. Численные результаты предсказывают явление "закупорки влаги" и взрывообразное растрескивание бетона в случае пожара. Исследования показывают, что применение уплотняющего слоя в качестве защиты от огня приводит к росту давления в порах бетонных стен, которое, в свою очередь, повышает чувствительность к вызываемым огнем повреждениям.